Fluorescence Quantum Yields of Laser Dyes Determined by On-Line Computer Evaluation

Günter Gauglitz, Alwin Lorch, and Dieter Oelkrug
Institut für Physikalische und Theoretische Chemie Tübingen

Z. Naturforsch. **37 a**, 219–223 (1982); received February 15, 1982

The determination of relative fluorescence quantum yields has been improved to better than 3% precision by use of a multichannel analyzer and an on-line desk-top computer. The new combined device for data acquisition and handling as well as a new correction procedure are described. Drifts of excitation source and dark current can be omitted. The yields for laser dyes, emitting at short wavelengths, are presented in dependence on excitation wavelength. These results simplify the optimal choice of the pump conditions of laser dyes, which usually are not photostable.

Introduction

In the past years dyes have been synthesized which show laser action in the wavelength range 400–450 nm or even below. But these dyes are not very photostable, which causes problems in case the pump intensities are very high, cw operation is wanted, or high reproducibility of the peak intensity is important. Recent publications show that the photostability of laser dyes drastically depends on the pump wavelength [1, 2]. A related dependence of the fluorescence quantum yield could be expected, since photochemical and fluorescence quantum yield together with the nonradiative desactivation result unite in most dyes. For this reason both photochemical and fluorescence quantum yield have to be determined in dependence on pump wavelengths in order to optimize pump conditions with respect to high laser output (which is related to highest possible fluorescence quantum yield) as well as low photodegradation (lowest possible photochemical quantum yield) of the dye solution.

The determination of absolute fluorescence quantum yields is known to be very tedious [3–6]. However, for many purposes it is sufficient to know the relative yields [4, 7, 8], especially if the results of similar dyes for various excitation wavelengths have only to be compared. Even in the case of the determination of relative yields, the literature refers to calculatory expenditure [7–9] because of the necessity for correction with respect to base line, dark current, and sensitivity. Therefore computers are recommended even for the measurement of a few samples [9, 10], not only for the intended serial determinations.

To meet these requirements, a fluorimeter system was combined with a multichannel analyzer; data were directly transferred to a minicomputer, and a SPLAUS curve fitting technique [11] together with a spectra correction method against drifts of light source and detector system were developed.

Experimental

The fluorimeter system (Carl Zeiss, Oberkochen) includes a xenon or mercury-arc source, two monochromators (M4 and MM12), the sample compartment ZFM4 and a photomultiplier RCA 7265 (S-20 cathode), operating in the photon counting mode. The anode pulses can be sampled in an Ortec counter modell 715, and stored in a mutlichannel analyzer (Ortec modell 6220). The output of the analyzer is transferred via a RS 232C interface (2400 baud) to a graphic display minicomputer TEK 4051 with a fast matrix printer LA 120, a plotter 4662 and external tape units 4924 (all Tektronix). A block diagram of the device is given in Figure 1. Quininesulfate in 1.0 N H_2SO_4 was used as a standard solution. Its absolute fluorescence quantum yield $\eta_s = 0.55$ was taken from the literature [8]. Both standard and sample absorbances were spectroscopically adjusted to equal absorbances ($A = 1$) at excitation wavelengths by use of 5 cm cells. These solutions were afterwards diluted according to the wavelength (absorbance

Reprint requests to Dr. G. Gauglitz, Institut f. Physikalische u. Theoret. Chemie Universität Tübingen, Auf der Morgenstelle 8, D-7400 Tübingen.

0340-4811 / 82 / 0300-0219 $ 01.30/0. — Please order a reprint rather than making your own copy.

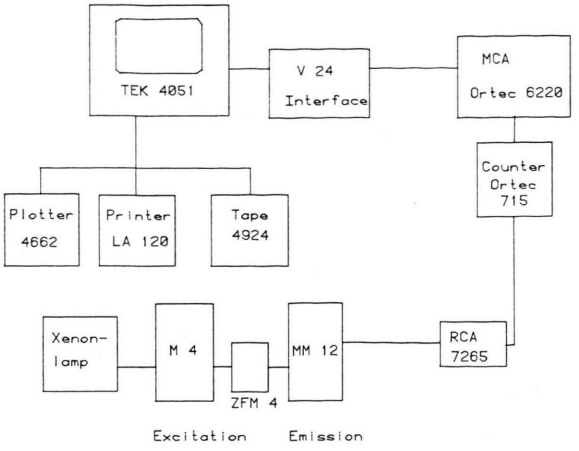

Fig. 1. Block diagram of the combined data sampling and handling device.

$A = 0.02$/cm at $\lambda > 254$ nm and $A = 0.1$/cm at $\lambda = 254$ nm). For two reasons the absorbances had to be increased at 254 nm: (a) the intensity of the light source is lower and (b) the absorptivities of the dyes are smaller compared to longer wavelengths. In fact, for some dyes the absorptivities were so small that the yields could not be measured without taking account for concentration quenching (see below), therefore they will not be listed. The „blank" was measured, too.

These experimental conditions guarantee the same losses by reflection and transmission, respectively, and equal geometry for both the sample and the standard. For these reasons errors by stray light, Raman emission by the solvent, and luminescence by the cell or impurities can be neglected. The highly diluted solutions (10^{-7} molar) can be expected to minimize effects by reabsorption and concentration quenching.

To get source intensities as high as possible the output of the combinations of xenon-lamp and monochromator was compared with that of the Hg-source and interference filter. The bandwidth of the excitation monochromator was kept smaller than 2 nm to avoid an influence of the spectral slit width of the entrance slit on the fluorescence yields [12, 13]. Four samples were measured during each experiment according to the following procedure:

The spectra were recorded between 13000 and 29000 cm^{-1} point by point every 200 cm^{-1}, one sample after the other. Higher resolution did not considerably increase the quality of the results. At each wavenumber the photomultiplier current was sampled 3 to 10 seconds and stored in the multichannel analyzer in dependence on the fluorescence intensity at the specific excitation wavelength. After these four series of intensity measurements,

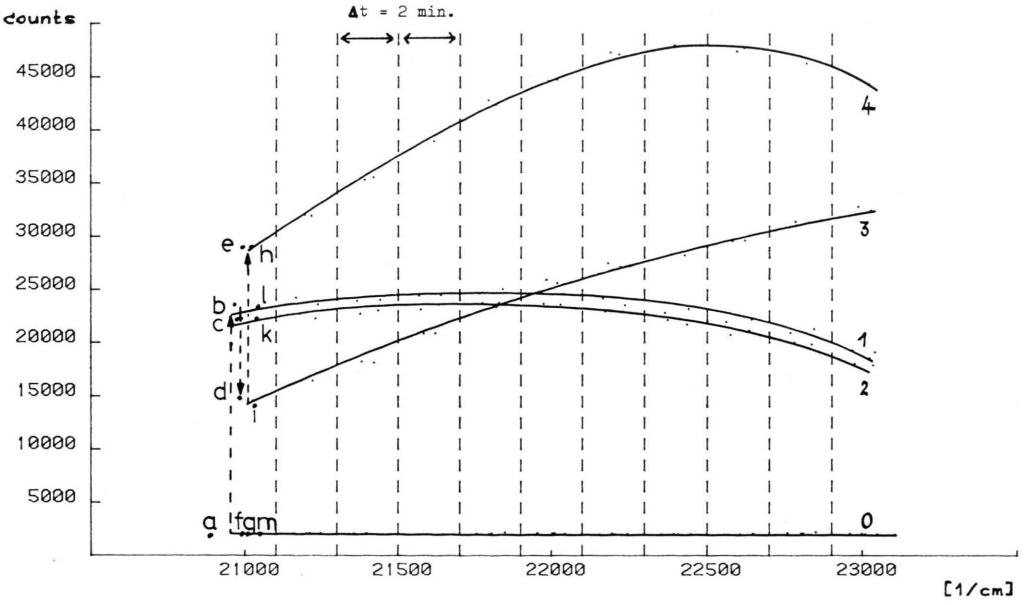

Fig. 2. Drift correction measurement at some emission wavenumbers in the region of the fluorescence peak. The small letters symbolize the procedure of measurement of the dark current (curve 0) and the four samples: quininesulfate 1 N (1), 0.1 N (2), stilbene-3 (3), coumarin 2 (4).

the values at only a few wavenumbers within the spectral maximum were measured within a short period of time for all four samples, to be able to correct for possible drifts of source intensity and dark current between the single series of measurements of the total spectra. This second part of the experiment is presented in Fig. 2, where the course of the procedure is symbolized by small letters at 21000 cm^{-1} for two laser dyes and two standard solutions. First the dark current is measured (a), then the four samples (b—e), twice the dark current again (f, g), the samples in opposite sequence (h—l) and finally the dark current (m) once more. Each of these cycles at one wavenumber takes about 2 minutes. These values are stored in the multichannel analyzer, too.

Evaluation Procedure

In case the absorbed light intensity

$$I_{abs} = I_0(1 - e^{-A}) \tag{1}$$

is known (A: absorbance, I_0: intensity of the excitation source), the fluorescence quantum yield η_F can be calculated using the area of the corrected fluorescence spectrum according to

$$F = \int_0^\infty I^F_{korr}(\tilde{\nu})\,d\tilde{\nu} = \eta_F I_{abs}. \tag{2}$$

$I^F_{korr}(\tilde{\nu})$ is the corrected fluorescence intensity at a specific wavenumber. If the excitation intensity I_0 and absorbance A for sample (x) and standard (s) are the same, $I_{abs}(x)$ and $I_{abs}(s)$ will be equal and the relative fluorescence quantum yield can be obtained by use of (1) as

$$\eta_F(x) = \eta_F(s)\,\frac{F_x}{F_s}\cdot\left(\frac{n_x}{n_s}\right)^2, \tag{3}$$

assuming inner filter effects to be negligible. If the solvents for the sample and the standard are different [7, 14], a correction becomes necessary with respect to the refractive indices n. By use of the fluorescence spectra of sample and standard and the intensity values at the emission maximum, taken within a short periode of time, the calculation of the fluorescence quantum yield proceeds in the following way:

Figure 3 shows the measured fluorescence spectrum of stilbene-3 in methanol (+) for excitation at 365 nm (small peak at 27400 cm^{-1}). The spectral distribution of the dark current is taken from a linear least squares fit through measurement points in wavelength regions where the sample does not emit. Dark current subtraction results in curve (□). This spectrum is corrected according to Lippert [15] by the stored spectral sensitivity curve $S(\tilde{\nu})$ of the fluorimeter-system (curve (×)). By use of a cubic

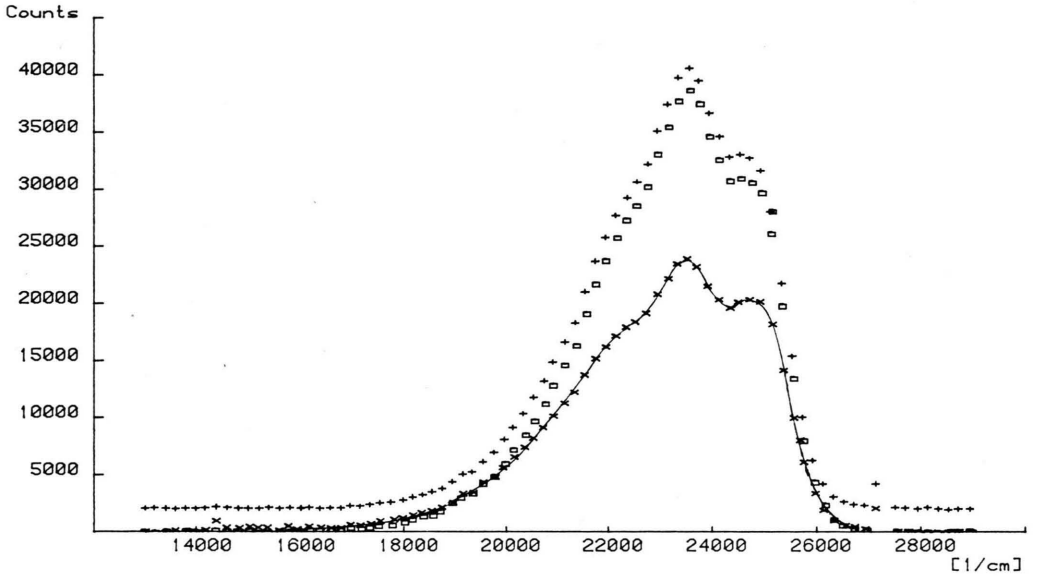

Fig. 3. Fluorescence spectrum of stilbene-3 in methanol after different steps of correction; excitation wavelength 365 nm.

Table 1. The area of the fluorescence spectrum for four samples. The eight columns refer to the different steps of correction.

	1	2	3	4	5	6	7	8
Quininesulfate (1 N H_2SO_4)	106159959	94872775	95126420	109555786	109415237	109549922	108859407	109418692
Quininesulfate (0.1 N H_2SO_4)	99223492	88382352	88530747	103233726	104118022	105182523	102739718	103794687
Stilbene-3 (methanol)	147600769	122436147	122707295	142712424	147109190	146755322	144971199	145892469
Coumarin 2 (methanol)	151903934	128146262	128303791	153512374	153540645	157230446	153912158	154975078

SPLAUS-algorithm [11, 16] the computer fits the data by a smooth curve using all spectral points. Thus the area of the fluorescence spectrum can be analytically integrated. The degree of fitting can be controlled during the calculation at the graphic display of the computer. The partial areas of the spectra are analogously handled. The original spectrum will be normalized by these correction values to become independent of the drift on the dark current. This can be done either by use of the smoothened intensity values at the maximum of the drift correction measurement or better by taking different sub-areas

$$F_T = \int_1^2 I^F_{korr}(\tilde{\nu})\,d\tilde{\nu}. \quad (4)$$

The advantage of the latter is, that by integration the noise of the measurement will be reduced. In Table 1 the results for four samples (quininesulfate in 1 N H_2SO_4 and 0.1 N H_2SO_4, stilbene-3 and coumarin in methanol) are given in counts after different steps of correction and evaluation:

Column (1): the measured spectrum, (2): this spectrum after dark current subtraction and correction according to [10], (3): after SPLAUS-smoothing, (4): after normalization by the peak intensity at 21800 cm^{-1}, (5): at 22000 cm^{-1}, (6): at 22200 cm^{-1}, (7): by the sub-area 21600—22400 cm^{-1}, and (8): by sub-area of 21200—22800 cm^{-1}. The corrections 4, 5, and 6 give very similar values. The best results with least standard deviation will be obtained by normalization of the sample- and standard-area by the sub-area between 21200 and 22800 cm^{-1} (column 8 in tab. 1, curve (—) in Figure 3). The use of too large a sub-area worsens the drift corrections.

Results and Discussion

Table 2 gives the relative fluorescence quantum yields of some laser dyes measured at four different excitation wavelengths. The values are based on an absolute yield of $\eta_F = 0.55$ for quininesulfate in 1 N H_2SO_4. The yield of quininesulfate in 0.1 N H_2SO_4 was also measured, to check the sensitivity and exactness of the evaluation method. The obtained value of 0.52 is in good accordance with the value discussed in literature [4, 17]. Each value of η_F in Table 2 was repeatedly reproduced within an accuracy of 1 to 3% according to the excitation wavelength. New dye solutions were prepared for each set of experiments. Great care had to be taken

Dyes (in methanol)	Excitation wavelength			
	365 nm	333 nm	313 nm	254 nm
DEMC [19]	0.40 ± 0.01	0.37 ± 0.01	0.39 ± 0.01	0.40 ± 0.02
CPTC	0.66 ± 0.02	0.70 ± 0.02	0.67 ± 0.01	0.72 ± 0.02
MMTC	0.80 ± 0.01	0.82 ± 0.02	0.78 ± 0.101	0.82 ± 0.02
TMTC	0.82 ± 0.01	0.82 ± 0.02	0.86 ± 0.03	—
MAPC	0.81 ± 0.02	0.85 ± 0.03	0.87 ± 0.03	—
Stilbene-1	0.60 ± 0.01	0.64 ± 0.02	0.58 ± 0.02	—
Stilbene-3	0.72 ± 0.01	0.75 ± 0.02	0.76 ± 0.02	—
Coumarin 2 [1]	0.77 ± 0.01	0.72 ± 0.02	0.73 ± 0.02	—
Coumarin 47	0.38 ± 0.02	0.44 ± 0.03	0.42 ± 0.02	—
Coumarin 120 [1]	0.71 ± 0.02	0.73 ± 0.02	—	—

Table 2. Fluorescence quantum yields of some laser dyes at different excitation wavelengths related to quininesulfate (1 N H_2SO_4, 298 K, $5 \cdot 10^{-3}$ molar).

to adjust all solutions to equal absorbances, particularly when the excitation wavelength corresponded to a shoulder in the absorption spectrum.

The absorptivities at short excitation wavelengths of some dyes are so small that the dye concentrations had to be very high to get reasonable sampling time for finite slit widths of the excitation and emission monochromators. Therefore problems by reabsorption and concentration quenching had to be expected and an evaluation was senseless.

Structure and nomenclature of the abbreviated laser dyes are given elsewhere [2, 18]. As marked in Table 2 some of the yields cited in the literature agree very well with our results.

Although the new correction and normalization procedure is very sophisticated, the computer extremely simplifies the evaluation. Besides, the sampling of data in the multichannel analyzer improves the S/N-ratio. For these reasons, the results for different excitation parameters can be compared.

The relative fluorescence quantum yields do not dpend on the excitation wavelength. This result is in contrast to that one of the photochemical quantum yields which strongly vary with excitation conditions [2]. This different behaviour is shown in Fig. 4 for three laser dyes. Of course the sum of all possible quantum yields of the photoexcited state normally adds up to one. Therefore an increase in the photochemical yield φ is supposed to cause a decrease in the fluorescence yield. But, φ turns out to be smaller than η_F by orders of magnitude. For this reason even drastic changes in φ are out of the error limits of an exact determination of the fluorescence quantum yield. Therefore the pump conditions in the laser system using these dyes can be optimized according to photostability considerations and absorptivity values.

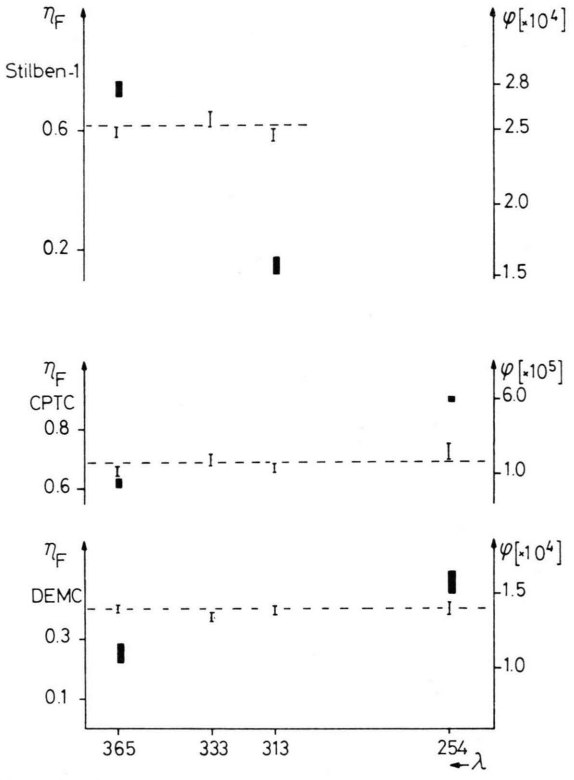

Fig. 4. Fluorescence (left axis) and photochemical (right axis) yields of three dyes. The error bars for the photochemical yields are indicated as rectangles ▮, the fluorescence ones as bars ⊥. The units of the left axis are the same for all dyes. The scalings of the photochemical yields differ.

Acknowledgement

We thank the Fonds der chemischen Industrie for financial support.

[1] A. N. Fletcher and D. E. Bliss, Appl. Phys. **16**, 289 (1978).
[2] G. Gauglitz, Z. Phys. Chem. Wiesbaden **113**, 217 (1978).
[3] C. A. Parker and W. T. Rees, Analyst. **85**, 587 (1960).
[4] J. N. Demas and G. A. Crosby, J. Phys. Chem. **75**, 991 (1971).
[5] W. H. Melhuish, J. Res. Nat. Bur. Stand. **76A**, 547 (1972).
[6] J. B. Birks, NBS Spec. Publ. **466**, 1 (1977).
[7] C. A. Parker, Photoluminescence of Solutions' Elsevier, Amsterdam 1968.
[8] W. H. Melhuish, J. Phys. Chem. **65**, 229 (1961).
[9] H. V. Drushel, A. L. Sommers, and R. C. Cox, Anal. Chem. **35**, 2166 (1963).
[10] J. E. Wampler and R. J. DeSa, Appl. Spectr. **25**, 623 (1971).
[11] H. Späth, Spline-Algorithmen, R. Oldenbourg Verlag, München 1973.
[12] A. N. Fletcher, Photochem. Photobiol. **9**, 439 (1969).
[13] J. Bendig, D. Kreysig, and R. Schöneich, Z. Chem. **19**, 151 (1979).
[14] J. J. Hermanns and S. J. Levinson, Opt. Soc. London **66A**, 921 (1953).
[15] E. Lippert, et al., Z. Analyt. Chem. **170**, 1 (1959).
[16] Ch. H. Reinsch, Num. Math. **10**, 177 (1967).
[17] W. R. Dawson and M. W. Windsor, J. Phys. Chem. **72**, 3251 (1968).
[18] D. Basting, F. P. Schäfer, and B. Steyer, Appl. Phys. **3**, 81 (1974).
[19] K. H. Drexhage, J. Res. NBS **80A**, 421 (1976).